

## Synthesis of Novel Quinacridone Dyes and Their Photovoltaic Performances in Organic Dye-sensitized Solar Cells

Chun Sakong, Se Hun Kim, Sim Bum Yuk, Jeong Yun Kim, Se Woong Park,<sup>†</sup> Min Jae Ko,<sup>†</sup> and Jae Pil Kim<sup>\*</sup>

Department of Materials Science and Engineering, Seoul National University, Seoul 151-744, Korea. \*E-mail: jaepil@snu.ac.kr  
<sup>†</sup>Solar Cell Research Center, Materials Science and Technology Division, Korea Institute of Science and Technology (KIST), Seoul 136-791, Korea

Received March 8, 2011, Accepted June 13, 2011

Two novel quinacridone (QNC) dyes with thiophene or benzene-conjugated bridge and cyanoacrylic acid acceptor were first designed and synthesized for use in dye-sensitized solar cells (DSSCs). The absorption spectra, electrochemical and photovoltaic properties of these dyes were investigated. Under simulated AM 1.5G irradiation conditions, the solar cell based on the quinacridone dye containing thiophene as a bridge unit had a short-circuit photocurrent density of 8.51 mA·cm<sup>-2</sup>, an open-circuit voltage of 643.6 mV, and a fill factor of 0.70, corresponding to an overall conversion efficiency of 3.86%.

**Key Words :** Quinacridone chromophore, Organic dyes, Dye-sensitized solar cell, Intramolecular charge transfer, Thiophene, Benzene

### Introduction

Dye-Sensitized Solar Cells (DSSCs) have attracted considerable attention in the field of renewable energy because of their easy processing, low production cost and high photoelectric conversion efficiency.<sup>1</sup> The most typical dyes used in DSSCs are the ruthenium(II) polypyridyl complex series, which are known as N3 and N719. These Ru-complex dyes showed photoelectric conversion efficiencies over 11%<sup>2</sup> and good long-term stability.<sup>3</sup> However, Ru-complex dyes have the disadvantage of high production cost and difficulties in purification. Recently, a variety of organic dyes have been developed as alternatives to Ru-complex dye.<sup>4</sup> They have the advantages of low cost, ease of structural changes, ease of synthesis and high molar extinction coefficients.

In this study, we report the design and synthesis of new organic dyes containing linear *trans*-quinacridone chromophores (QNC).<sup>5</sup> These chromophores have been studied for photovoltaic and photoconductive substances<sup>6,7</sup> and have excellent durability as well as effective absorption in the 500-550 nm region.<sup>8</sup> These new quinacridone dyes were composed of N-butylated quinacridone as a donor, a thiophene or benzene as a conjugated bridge and cyanoacrylic acid as the acceptor and anchoring group. In designing dyes, two butyl groups were introduced at the N atom of quinacridone to improve its solubility.<sup>7,9</sup> In addition, a thiophene or benzene was introduced as a bridge unit to facilitate the synthesis because direct formylation employing Vilsmeier reagent (POCl<sub>3</sub>) is difficult due to the carbonyl group included in quinacridone.<sup>10</sup>

### Experimental Section

**Materials and Methods.** Quinacridone, 1-bromobutane,

hexadecyltrimmonium bromide and 4-formylphenyl boronic acid purchased from TCI, benzyltrimethylammonium tribromide, 5-formyl-2-thiophene boronic acid, tetrakis(triphenylphosphine)palladium(0), cyanoacetic acid and piperidine from Sigma-Aldrich were used without further purification. <sup>1</sup>H NMR spectra were recorded by Bruker Avance 500 at 500 MHz using CDCl<sub>3</sub> and MeOD as the solvent and TMS as the internal standard. Mass spectra were measured with JEOL JMS-600W Agilent 6890 Series. UV-Visible absorption spectra were measured with an HP 8452A spectrophotometer and emission spectra were recorded on a QuantaMaster™ UV VIS spectrofluorometer. Cyclic voltammetry (CV) was performed with a three-electrode electrochemical cell on a Potentostat/Gavanostat Model 273A. Glassy-carbon, platinum wire, and Ag/Ag<sup>+</sup> were employed as working, counter, and reference electrodes, respectively. Tetrabutylammonium tetrafluoroborate (TBATFB) was used as the supporting electrolyte and ferrocene was added as the internal reference for calibration.

#### Synthesis of Dyes.

**5,12-Dibutylquinacridone (1):** A suspension of quinacridone (1.56 g, 5 mmol), hexadecyltrimmonium bromide (TBAB, 1.822 g, 5 mmol), toluene (160 mL) and 50% aqueous potassium hydroxide (50 g) was vigorously stirred and heated at 95 °C. When quinacridone had completely dissolved, 1-bromobutane (2.16 mL, 20 mmol) was added and the mixture was vigorously stirred for 24 hrs. And then the mixture was cooled to room temperature and poured slowly into ice water. The mixture was neutralized with 10% HCl solution and the crude product was extracted with methylene chloride. The organic layer was washed with water and brine, dried over anhydrous MgSO<sub>4</sub>. The solvent was removed by rotary evaporation and subsequently dried in a vacuum oven. The crude product was purified by column chromatography on silica gel using methylene chloride. The yields, <sup>1</sup>H NMR

and Mass data are given below.

Yield: 80% (1.7 g).  $^1\text{H NMR}$  ( $\text{CDCl}_3$ )  $\delta$  8.78 (s, 2H), 8.58 (d, 2H), 7.77 (t, 2H), 7.52 (d, 2H), 7.28 (t, 2H), 4.52 (t, 4H), 2.01 (m, 4H), 1.67 (m, 4H), 1.12 (m, 6H). FAB MS:  $m/z$  425  $[\text{M}^+]$ . Anal. Calc. for  $\text{C}_{28}\text{H}_{28}\text{N}_2\text{O}_2$ : C, 79.22; H, 6.65; Found: C, 79.01; H, 6.37.

**2-Bromo-5,12-dibutylquinacridone (2):** 5,12-Dibutylquinacridone (**1**) (1.68 g, 3.5 mmol) was mixed with ethanol (80 mL) and benzyltrimethylammonium tribromide (BTA-TB, 1.77 g, 4.5 mmol). The resulting mixture was stirred at ambient temperature for 24 hrs, and then heated at 85 °C for 20 hrs to give limited reaction. Addition of chloroform (100 mL) dissolved all solids and continued reflux gave moderate generation of mono- and di-brominated products. After evaporation of solvent, the product was purified by column chromatography on silica gel using methylene chloride.

Yield: 51% (0.88 g).  $^1\text{H NMR}$  ( $\text{CDCl}_3$ )  $\delta$  8.67 (s, 1H), 8.63 (s, 1H), 8.57 (s, 1H), 8.49 (d, 1H), 7.73-7.71 (m, 2H), 7.46 (d, 1H), 7.34 (d, 1H), 7.22 (m, 1H), 4.46 (m, 4H) 1.97-1.93 (m, 4H), 1.3-1.11 (m, 6H). FAB MS:  $m/z$  503  $[\text{M}^+]$ . Anal. Calc. for  $\text{C}_{28}\text{H}_{27}\text{BrN}_2\text{O}_2$ : C, 66.80; H, 5.41; Found: C, 66.64; H, 5.21.

**5-(5,12-Dibutyl-7,14-dioxo-7,14-dihydro-12H-quinol[2,3-b]acridine-2-yl)thiophene-2-carbaldehyde (3a):** 2-Bromo-5,12-dibutylquinacridone (**2**) (0.76 g, 1.5 mmol) was dissolved in a mixture (7:3) of dry toluene and ethanol (75 mL) and the solution was purged with argon gas for 10 min. Tetrakis(triphenylphosphine)palladium(0) (0.086 g, 0.075 mmol) was added followed by 5-formyl-2-thiophene boronic acid (0.26 g, 1.66 mmol) and a 2 M aqueous potassium carbonate solution (3 mL). The reaction mixture was heated at 110 °C for 12 hrs and then cooled to room temperature. The organic solvents were evaporated under vacuum, and the residue was extracted with methylene chloride and water, washed with water and brine, and dried over anhydrous  $\text{MgSO}_4$ . The solvent was removed by rotary evaporation and subsequently dried in a vacuum oven. The crude product was purified by column chromatography on silica gel using methylene chloride.

Yield: 35% (0.28 g).  $^1\text{H NMR}$  ( $\text{CDCl}_3$ )  $\delta$  9.92 (s, 1H), 8.91 (s, 1H), 8.83 (d, 2H), 8.61 (d, 1H), 8.06 (d, 1H), 7.80 (d, 2H), 7.70 (t, 1H), 7.62 (d, 1H), 7.55 (d, 1H), 7.32 (m, 1H), 4.57 (m, 4H), 2.03 (m, 4H), 1.68 (m, 4H), 1.14 (m, 6H). FAB MS:  $m/z$  535  $[\text{M}^+]$ . Anal. Calc. for  $\text{C}_{33}\text{H}_{30}\text{N}_2\text{O}_3\text{S}$ : C, 74.13; H, 5.66; Found: C, 73.95; H, 5.45.

**2-Cyano-3-(5-(5,12-dibutyl-7,14-dioxo-7,14-dihydro-12H-quinol[2,3-b]acridine-2-yl)thiophene-2-yl) Cyanoacrylic Acid (QNC-1):** A mixture of the carbaldehyde (**3**) (0.27 g, 0.5 mmol), cyanoacetic acid (0.11 g 1.25 mmol) and piperidine (0.15 mL, 1.5 mmol) was dissolved in acetonitrile (150 mL) and gently heated at 92 °C for 8 hrs under nitrogen. After removal of solvent in vacuum, the crude product was purified by column chromatography on silica gel using chloroform/methanol (5:1, v/v).

Yield: 54% (0.162 g).  $^1\text{H NMR}$  (MeOD)  $\delta$  8.55 (s, 1H), 8.51 (d, 2H), 8.28 (d, 2H), 8.01 (d, 1H), 7.89 (s, 1H), 7.84 (d, 1H), 7.70 (t, 1H), 7.60 (m, 2H), 7.49 (d, 1H), 4.54 (m, 4H),

2.03 (m, 4H), 1.68 (m, 4H), 1.14 (m, 6H). FAB MS:  $m/z$  602  $[\text{M}^+]$ . Anal. Calc. for  $\text{C}_{36}\text{H}_{31}\text{N}_3\text{O}_4\text{S}$ : C, 71.86; H, 5.19; Found: C, 71.68; H, 4.98.

**Compound 3b:** This compound was prepared using the method established for **3a**.

Yield: 42% (0.31 g).  $^1\text{H NMR}$  ( $\text{CDCl}_3$ )  $\delta$  10.08 (s, 1H), 8.87 (s, 1H), 8.79 (d, 2H), 8.57 (d, 1H), 8.05 (d, 1H), 8.01 (d, 2H), 7.90 (d, 2H), 7.75 (t, 1H), 7.64 (d, 1H), 7.53 (d, 1H), 7.29 (m, 1H), 4.57 (m, 4H), 2.03 (m, 4H), 1.68 (m, 4H), 1.14 (m, 6H). FAB MS:  $m/z$  529  $[\text{M}^+]$ . Anal. Calc. for  $\text{C}_{35}\text{H}_{32}\text{N}_2\text{O}_3$ : C, 79.52; H, 6.10; Found: C, 79.34; H, 5.87.

**QNC-2:** This compound was prepared using the method established for **QNC-1**.

Yield: 56% (0.165 g).  $^1\text{H NMR}$  ( $\text{CDCl}_3$ )  $\delta$  8.65 (s, 2H), 8.64 (d, 1H), 8.35 (d, 1H), 8.23 (d, 1H), 8.01 (d, 2H), 7.97 (d, 1H), 7.96 (t, 1H), 7.90 (d, 2H), 7.84 (d, 2H), 7.30 (s, 1H), 4.59 (m, 4H), 1.89 (m, 4H), 1.62 (m, 4H), 1.08 (m, 6H). FAB MS:  $m/z$  596  $[\text{M}^+]$ . Anal. Calc. for  $\text{C}_{38}\text{H}_{33}\text{N}_3\text{O}_4$ : C, 76.62; H, 5.58; Found: C, 76.43; H, 5.46.

**Fabrication of Solar Cells and Photovoltaic Measurement:** FTO glass plates (Pilkington, TEC-8, 8  $\Omega$ /square, 2.3 mm thick) were cleaned with ethanol by ultrasonication for 10 min, and then treated in a UV- $\text{O}_3$  system for 20 min. The FTO layer was first covered with 7.5% Ti(IV) bis(ethyl acetoacetato)-diisopropoxide solution by spin-coating method. For the transparent nanocrystalline layer,  $\text{TiO}_2$  paste (230(M2331)-2T) was coated on the FTO glass plates by doctor blade printing, and then sintering was carried out at 500 °C for 30 min.  $\text{TiO}_2$  paste (CCIC-IT) for the scattering layer was prepared using the same method. The resulting layer was composed of 9  $\mu\text{m}$  thickness of transparent layer and 4  $\mu\text{m}$  thickness of scattering layer. Active area of  $\text{TiO}_2$  films was about 0.23  $\text{cm}^2$ . The  $\text{TiO}_2$  electrodes were immersed into the dye solution (0.5 mM in chloroform-methanol (1:1) solution) and kept at room temperature for 40 hrs. Counter electrodes were prepared by dropping a 0.7 mM  $\text{H}_2\text{PTCl}_6$  solution on a FTO glasses and heating at 400 °C for 20 min. The dye-absorbed  $\text{TiO}_2$  electrode and the counter electrode were sealed using 25  $\mu\text{m}$ -thick surlin film (Dupont 1702). An electrolyte solution was introduced through a drilled hole on the counter electrode, where the electrolyte solution was consisted of 0.5 M 1-methyl-3-propylimidazolium iodide (PMII), 0.2 M LiI, 0.05 M  $\text{I}_2$ , and 0.5 M 4-tert-butylpyridine (TBP) in ACN/VN (85:15). Photovoltaic measurements were performed using a Keithly model 2400 source measuring unit. A 1000W Xe lamp (Spectra-physics) served as a light source and its light intensity was adjusted using a NREL-calibrated silicon solar cell equipped with a KG-5 filter to approximate AM 1.5G of sun light intensity. IPCE was measured as a function of wavelength from 300-800 nm using a specially designed IPCE system for dye-sensitized solar cells (PV Measurements, Inc.). A 75W Xe lamp was used as the light source for generation of a monochromatic beam. Calibrations were performed using a silicon photodiode, which was calibrated using NIST-calibrated photodiode G425 as a standard, and IPCE values were collected at a low chopping speed of 10 Hz.

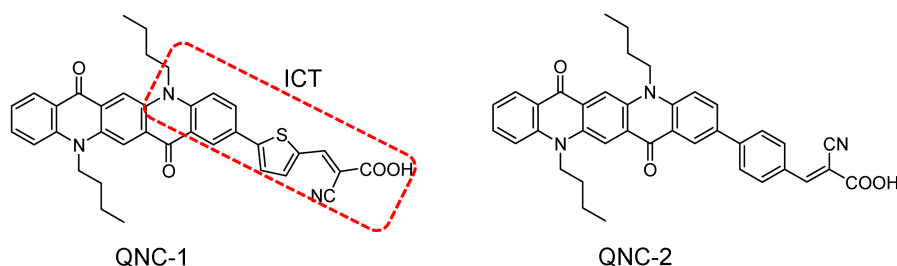


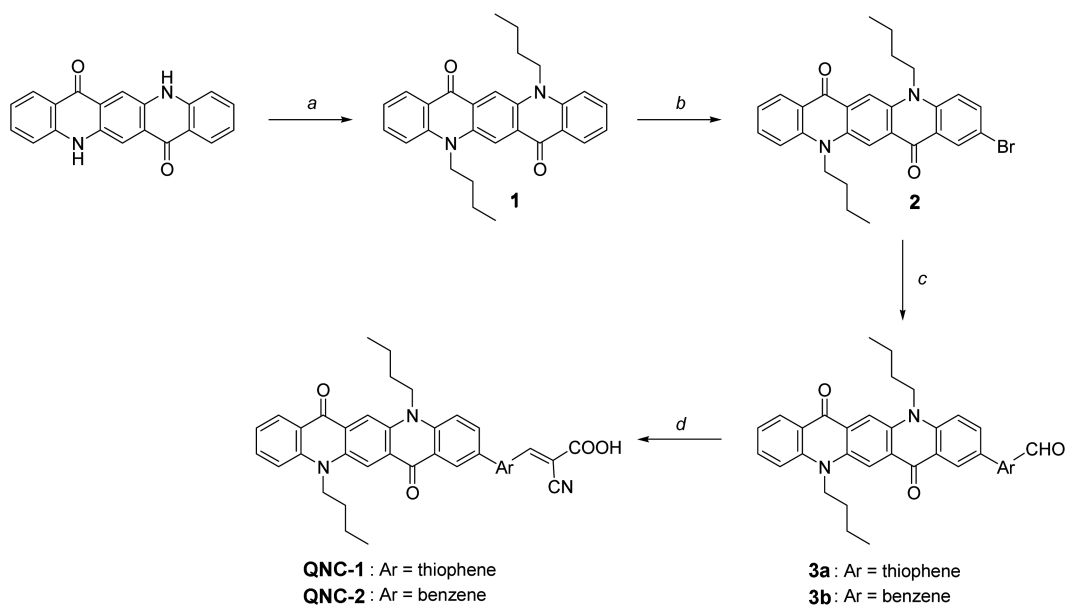
**Figure 1.** Molecular structures of **QNC-1** and **QNC-2**.

## Results and Discussion

**Synthesis of Dyes.** Molecular structures of the synthesized dyes are as shown in Figure 1 and their synthetic routes are illustrated in Scheme 1. Firstly, *N*-butylation of quinacridone<sup>9</sup> was carried out to improve its solubility in organic solvents such as dichloromethane, chloroform, toluene, ethyl acetate, *etc.* Secondly, the quinacridone was brominated at the 2-position with BTA-TB (benzyltrimethylammonium tribromide) for the synthesis of asymmetric quinacridone.<sup>11</sup> A mono-brominated quinacridone was coupled with 5-formyl-2-thiophene boronic acid or 4-formylphenyl boronic acid under Suzuki coupling conditions<sup>12</sup> and finally condensed with cyanoacrylic acid.

**Optical Properties of QNC Dyes in Solution and TiO<sub>2</sub> Film.** Figure 2(a) shows the UV-Visible absorption spectra of intermediate **1**, **QNC-1** and **QNC-2**, and their optical properties are collected in Table 1. The spectrum of the intermediate **1** shows single absorption band corresponding to a localized aromatic  $\pi$ - $\pi^*$  transition at 530 nm. As shown in Figure 1, **QNC-1** and **QNC-2** exhibit two prominent absorption bands at 414 nm/538 nm and 384 nm/536 nm, respectively. The absorption bands at the longer wavelength

are due to the localized aromatic  $\pi$ - $\pi^*$  transition and red-shifted from that of intermediate **1** only 6–8 nm when a bridge and an anchoring group were introduced. On the other hand, the strong absorption bands at the shorter wavelength red-shifted considerably, approximately 74 nm and 44 nm. Moreover, the molar extinction coefficients of the dyes at these wavelengths also increased dramatically compared to that of the localized aromatic  $\pi$ - $\pi^*$  transition. It is well known that the introduction of electron-withdrawing groups or an expansion of the conjugation length in dye structure generally produces intramolecular charge transfer (ICT) between the donor part of the molecule and the acceptor group with a strong red-shifted absorption band and increased intensity.<sup>13</sup> Therefore, the strong absorption band at the shorter wavelength can be assigned to the intramolecular charge transfer band. This assignment is also supported by solvatochromic behavior of the dyes. As shown in Figure 2(b), the aromatic  $\pi$ - $\pi^*$  transition band at 538 nm are nearly solvent polarity independent, whereas the intramolecular charge transfer band at 414 nm exhibits negative solvatochromism, i.e., blue shift of  $\lambda_{\text{max}}$  in more polar solvents. In general, the intramolecular charge transfer band of organic dye with D- $\pi$ -A structure appears at longer wavelength than



**Scheme 1.** Synthetic routes for the synthesis of QNC dyes; (a) 1-bromobutane, hexadecyltrimonium bromide, KOH, reflux in toluene (b) benzyltrimethylammonium tribromide, ethanol, room temp.  $\rightarrow$  reflux (c) 5-formyl-2-thiophene boronic acid or 4-formylphenyl boronic acid, tetrakis(triphenylphosphine)palladium(0), toluene:ethanol (7:3), reflux (d) cyanoacetic acid, piperidine, reflux in acetonitrile.

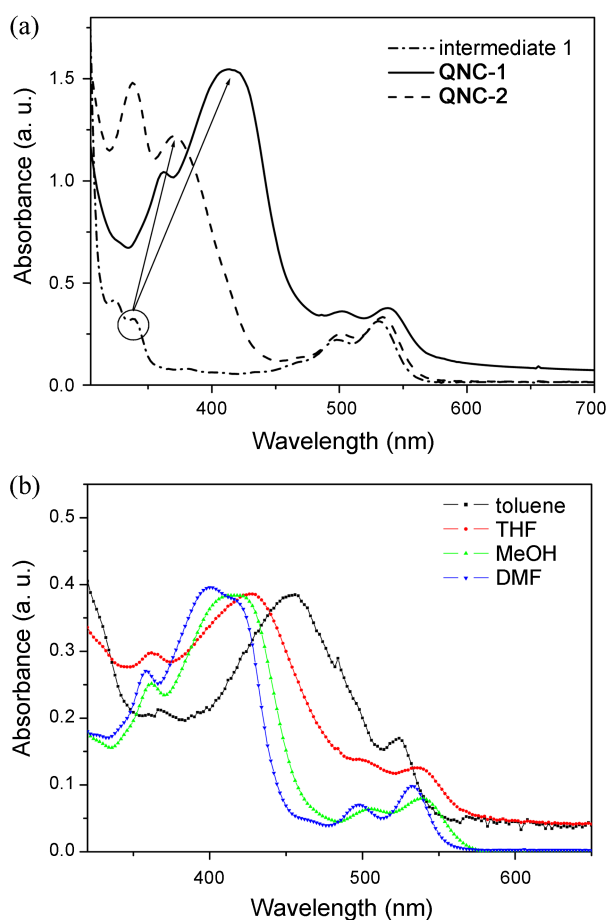


**Figure 2.** Absorption spectra of intermediate **1**, **QNC-1** and **QNC-2** in methanol (a) and absorption spectra of **QNC-1** in different solvents (b).

**Table 1.** Optical and electrochemical properties of **QNC-1** and **QNC-2**

Dye	$\lambda_{\text{max}}^a/\text{nm}$ ( $\epsilon/\text{M}^{-1}\text{cm}^{-1}$ )	$\lambda_{\text{max}}$ on $\text{TiO}_2/\text{nm}$	Potentials and energy levels		
			$E_{\text{ox}}^b/\text{V}$	$E_{0,0}^c/\text{V}$	$E_{\text{ox}}-E_{0,0}/\text{V}$
QNC-1	414 (45,200)	426	1.14	2.17	-1.03
	538 (15,100)				
QNC-2	384 (38,500)	414	1.21	2.21	-1.00
	536 (12,600)				

<sup>a</sup>Absorption maxima in methanol solution. <sup>b</sup>The oxidation potentials ( $E_{\text{ox}}$ ) of the dyes were obtained by cyclic voltammetry in  $\text{CH}_2\text{Cl}_2$  with 0.1 M tetrabutylammonium tetrafluoroborate (TBATFB) with a scan rate of  $100 \text{ mV}\cdot\text{s}^{-1}$  and converted to NHE. <sup>c</sup> $E_{0,0}$  of dyes were estimated from the edge of absorption spectra.

the localized  $\pi-\pi^*$  transition band. But, in case of QNC dyes, the intramolecular charge transfer band appeared at shorter wavelength than the localized  $\pi-\pi^*$  transition band. It is considered that only the benzene ring containing *N*-butyl group in quinacridone is included in conjugation with anchoring group, resulting in shorter conjugation path for intramolecular charge transfer with shorter absorption wavelength compared with the localized  $\pi-\pi^*$  transition band.

**QNC-1** bearing thiophene as the conjugated bridge showed a larger and stronger red-shift in the intramolecular charge transfer band compared to **QNC-2**. This is consider-

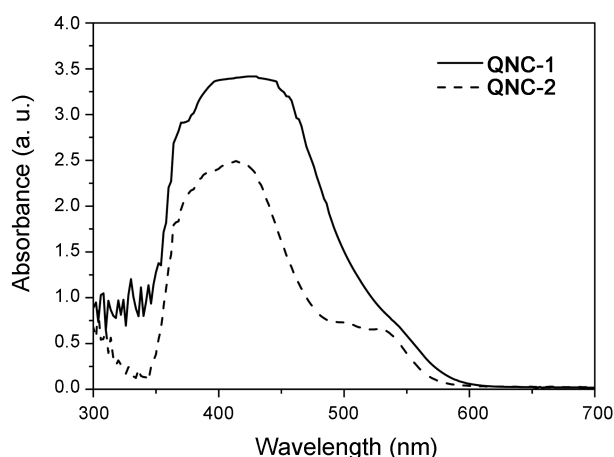


**Figure 3.** Absorption spectra of **QNC-1** and **QNC-2** adsorbed on  $\text{TiO}_2$ .

ed due to the different resonance stabilization energy of bridge unit and coplanarity of dye molecule. It has been known that a thiophene has a lower energy of charge transfer transition<sup>14</sup> because of its smaller resonance stabilization energy (thiophene, 29 Kcal/mol; benzene, 36 Kcal/mol) compared with a benzene.<sup>15</sup> Also, the thiophene can provide more effective conjugation due to its better coplanarity with quinacridone donor. As shown in Figure 7(a), the dihedral angles between quinacridone donor and bridge unit for **QNC-1** and **QNC-2** are  $19.8^\circ$  and  $33.6^\circ$ , respectively. This red-shift in the absorption spectrum could improve the amount of light harvested and enhance the photocurrent generation of DSSCs.

Figure 3 shows the absorption spectra of **QNC-1** and **QNC-2** on  $\text{TiO}_2$  films. As shown in Figure 3, the absorption maxima of intramolecular charge transfer bands for **QNC-1** and **QNC-2** on the  $\text{TiO}_2$  films were at 426 nm and 414 nm, which red-shifted by 12 nm and 30 nm compared with those in methanol, respectively.<sup>16</sup> The  $\pi-\pi^*$  transition bands of the dyes weakly appeared around 500–550 nm.

**Electrochemical Properties of QNC Dyes.** The oxidation potential ( $E_{\text{ox}}$ ) corresponding to the HOMO level of the dye

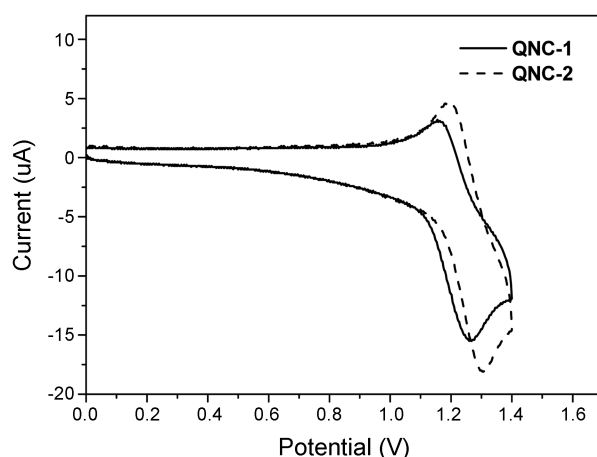


**Figure 4.** Cyclic voltammograms of **QNC-1** and **QNC-2**.

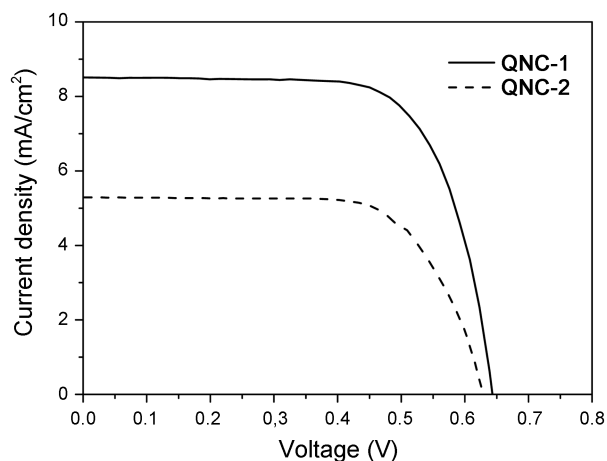
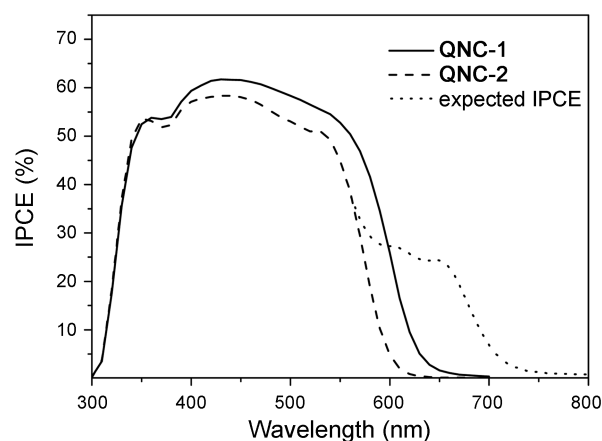
**Table 2.** Photovoltaic properties of QNC-1 and QNC-2

Dye	Photovoltaic performance data <sup>a</sup>			
	$J_{sc}/\text{mA}\cdot\text{cm}^{-2}$	$V_{oc}/\text{mV}$	FF	$\eta$ (%)
QNC-1	8.51	643.6	0.70	3.86
QNC-2	5.29	629.1	0.69	2.30

<sup>a</sup>The concentration was maintained at  $5 \times 10^{-4}$  M in chloroform-methanol (1:1) solution, with 0.5 M 1-methyl-3-propylimidazolium iodide (PMI), 0.2 M LiI, 0.05 M  $I_2$  and 0.5 M 4-tert-butylpyridine (TBP) in ACN-VN (85:15) solution. Performance of DSSC was measured with a  $0.23 \text{ cm}^2$  working area.

was obtained from cyclic voltammetry (CV) and the LUMO level was calculated by  $E_{ox}-E_{0-0}$ . The  $E_{0-0}$  is the zeroth-zeroth energy of the dye determined from the inflection point at the end of the visible absorption spectrum of the dye.<sup>17</sup> The cyclic voltammograms of the synthesized dyes are shown in Figure 4 and corresponding data are collected in Table 1. The oxidation potentials of QNC-1 and QNC-2 were 1.14 eV and 1.21 eV, respectively, which are more positive than the redox potential of the electrolyte (0.4 eV vs NHE). The LUMO levels of QNC-1 and QNC-2 were  $-1.03$  eV and  $-1.00$  eV, respectively, which are more negative than the conduction band of  $\text{TiO}_2$  ( $-0.5$  eV vs NHE).<sup>18</sup> Therefore, the HOMO-LUMO levels of the synthesized dyes were suitable for DSSCs to be driven.

**Photovoltaic Properties of DSSCs.** DSSCs were fabricated using the synthesized dyes according to the methods described in the Experimental section. The photovoltaic performances of these DSSCs are listed in Table 2, and the respective photocurrent density-voltage (J-V) curves are shown in Figure 5. Under standard AM 1.5 G irradiation, the maximum efficiency ( $\eta$ ) for the QNC-1-sensitized solar cell with an active area of  $0.23 \text{ cm}^2$  was calculated to be 3.86%, with a short-circuit current ( $J_{sc}$ ) of  $8.51 \text{ mA}\cdot\text{cm}^{-2}$ , an open-circuit voltage ( $V_{oc}$ ) of 643.6 mV and a fill factor (ff) of 0.70. On the other hand, the DSSCs based on QNC-2 showed a relatively lower  $J_{sc}$ , leading to a lower  $\eta$  value of 2.3%. This was attributed to the more red-shifted and broader absorption spectrum of QNC-1 bearing a thiophene as a conjugated

**Figure 5.** Photocurrent-voltage curves for the DSSCs based on QNC-1 and QNC-2 under AM 1.5 G simulated solar light ( $100 \text{ mW}\cdot\text{cm}^{-2}$ ).**Figure 6.** Incident photon-to-current conversion efficiencies spectra for the DSSCs based on QNC-1 and QNC-2.

bridge than that of QNC-2 bearing a benzene.

Figure 6 shows the incident monochromatic photon-to-current conversion efficiencies (IPCE) of the DSSCs based on the QNC dyes. The range of the IPCE spectrum based on QNC-1 was up to 670 nm with the highest value of 61.74% at 430 nm. On the other hand, the range of the IPCE spectrum based on QNC-2 was up to 625 nm, and it exhibited a lower IPCE with a maximum of 58.33% at 430 nm. The rather low IPCE value for QNC-2 indicates a lower photocurrent and inferior photovoltaic performance.

The IPCE spectrum generally reflects the corresponding absorption spectrum of a dye on  $\text{TiO}_2$  film and its onset usually expands approximately 200 nm compared to that of the absorption spectrum of the dye.<sup>19</sup> However, in the case of QNC dyes, the IPCE spectra didn't correspond with the absorption spectra of the dyes on  $\text{TiO}_2$  films and did not fully red-shifted as expected. The absorption bands at shorter wavelength (426 nm and 414 nm) of the QNC dyes were reflected in the IPCE spectra, but those of the longer wavelength above 500 nm were not. If the absorption bands at a longer wavelength were used to generate the photocurrent, the onset of the IPCE spectrum should have been expanded up to 750 nm. This means that only absorption bands due to the intramolecular charge transfer, occurring between the *N*-butyl group at the quinacridone donor and cyanoacrylic acid acceptor, contributed to the monochromatic incident photon-to-current conversion efficiency. We postulate that the two carbonyl groups on quinacridone framework with intense electron-withdrawing property compete with cyanoacrylic acid anchoring group and prevent the transfer of localized electrons in the quinacridone moiety resulting no contribution of longer absorption wavelength to IPCE.

**Computational Study.** All calculations were done by the Gaussian 09 program. The molecular geometry and the electron distributions of the synthesized dyes for the HOMO and LUMO state were calculated with DFT on a B3LYP/6-31+G(d) level. The electron densities in the HOMO states were higher at *N*-butyl groups on quinacridone framework, but they effectively shifted toward the anchoring group in

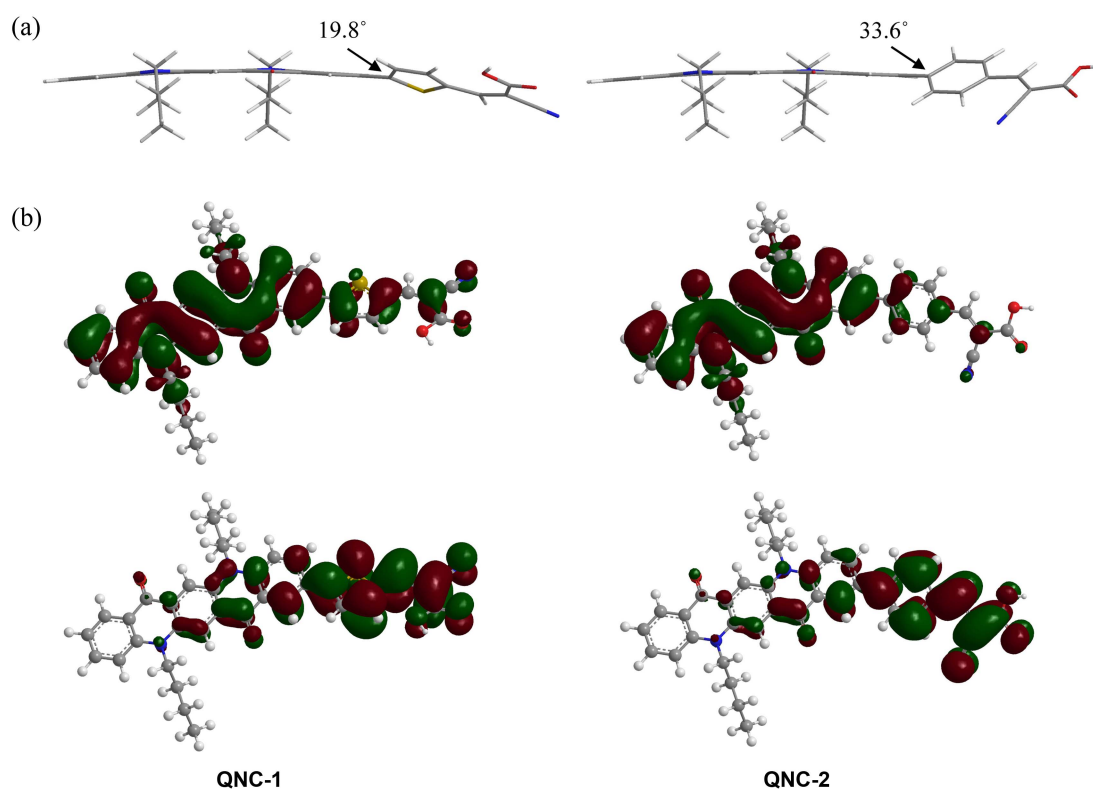


**Figure 7.** Optimized molecular geometry (a) and frontier molecular orbitals of the HOMO and LUMO (b) calculated with DFT on a B3LYP/6-31+G(d) level of QNC dyes.

the LUMO states. It is considered that the electron transfer from *N*-butyl group on the quinacridone framework to the anchoring group easily occurred by introduction of cyanoacrylic acid group as a stronger acceptor and anchoring group. As a result, the quinacridone dyes have superior photovoltaic performances compared to those of anthraquinone<sup>20</sup> and perylene dyes,<sup>21</sup> although they have two carbonyl groups with the strong electron-withdrawing character on framework.

### Conclusion

We have first designed and synthesized two novel quinacridone dyes with thiophene or benzene-conjugated bridge and cyanoacrylic acid acceptor and applied them to DSSCs. The intramolecular charge transfer bands of QNC dyes appeared at shorter wavelength than the localized  $\pi$ - $\pi^*$  transition bands due to shorter conjugation path (from *N*-butyl to anchoring group) for intramolecular charge transfer. The photovoltaic measurements showed that two quinacridone dyes had rather low overall conversion efficiency, which was 3.86% and 2.3%, respectively. We found that such lower conversion efficiency is due to the two carbonyl groups on quinacridone framework with intense electron-withdrawing property, which compete with cyanoacrylic acid anchoring group and prevent the transfer of localized electrons in the quinacridone moiety resulting contribution of only shorter absorption wavelength to IPCE. Although

quinacridone dyes have good durability and high molar extinction coefficients, further structural modification to move the residual electrons from the quinacridone moiety to the anchoring group is needed to improve their performance in DSSCs.

**Acknowledgments.** This work was supported by the Korea Evaluation Institute of Industrial Technology grant funded by the Korea government (MKE).

### References

- (a) O'Regan, B.; Grätzel, M. *Nature* **1991**, 353, 737. (b) Grätzel, M. *Nature* **2001**, 414, 338.
- (a) Chiba, Y.; Islam, A.; Watanabe, Y.; Komiyama, R.; Koide, N.; Han, L. *Jpn. J. Appl. Phys.* **2006**, 45, L638. (b) Nazeeruddin, M. K.; Angelis, F. D.; Fantacci, S.; Selloni, A.; Viscardi, G.; Liska, P.; Ito, S.; Takeru, B.; Grätzel, M. *J. Am. Chem. Soc.* **2005**, 127, 16835. (c) Wang, Z.-S.; Yamaguchi, T.; Sugihara, H.; Arakawa, H. *Langmuir* **2005**, 21, 4272.
- Wang, P.; Zakeeruddin, S. M.; Moser, J. E.; Nazeeruddin, M. K.; Sekiguchi, T.; Grätzel, M. *Nat. Mater.* **2003**, 2, 402.
- Mishra, A.; Fischer, M. K.; Bäuerle, P. *Angew. Chem., Int. Ed.* **2009**, 48, 2474.
- (a) Labana, S. S.; Lababa, L. L. *Chem. Rev.* **1967**, 67, 1. (b) Herbst, W.; Hunger, K. *Industrial Pigments*; VCH: Weinheim, 1993; 447. (c) Lincke, G. *Dyes and Pigments* **2002**, 52, 169.
- (a) Manabe, K.; Kusabayashi, S.; Yokoyama, M. *Chem. Lett.* **1987**, 609. (b) Marco, P. D.; Fattori, V.; Giro, G.; Kalinowski, J. *Mol. Cryst. Liq. Cryst.* **1992**, 217, 223. (c) Tsutsui, T.; Aminaka, E.; Fujita, Y.; Hamada, Y.; Saito, S. *Synth. Met.* **1993**, 57, 4157.

- (d) Shi, J.; Tang, C. W. *Appl. Phys. Lett.* **1997**, *70*, 1665. (e) Jabbour, G. E.; Kawabe, Y.; Shaheen, S. E.; Wang, J. F.; Morrell, M. M.; Kippelen, B.; Peyghambarian, N. *Appl. Phys. Lett.* **1997**, *71*, 1762. (f) Feyter, S. D.; Gesquière, A.; Schryver, F. C. D.; Keller, U.; Müllen, K. *Chem. Mater.* **2002**, *14*, 989. (g) Mu, Z.; Wang, Z.; Zhang, X.; Ye, K.; Wang, Y. *J. Phys. Chem. B* **2004**, *108*, 19955. (h) Yang, X.; Mu, Z.; Wang, Z.; Zhang, X.; Wang, J.; Wang, Y. *Langmuir* **2005**, *20*, 7225.
7. (a) Ortiz, A.; Flora, W. H.; D'Ambruoso, G. D.; Armstrong, N. R.; McGrath, D. V. *Chem. Commun.* **2005**, 444. (b) Liu, J.; Gao, B.; Cheng, Y.; Xie, Z.; Geng, Y.; Wang, L.; Jing, X.; Wang, F. *Macromolecules* **2008**, *41*, 1162.
8. Sakong, C.; Kim, Y. D.; Choi, J.-H.; Yoon, C.; Kim, J. P. *Dyes and Pigments* **2011**, *88*, 166.
9. (a) Liu, P. H.; Tian, H.; Chang, C. P. *J. Photochem. Photobiol. A* **2000**, *137*, 99. (b) Smith, J. A.; West, R. M.; Allen, M. *J. Fluoresc.* **2004**, *14*, 151.
10. Marson, C. M. *Tetrahedron* **1992**, *48*, 3659.
11. Smith, J. A. inventor; GE Healthcare UK Limited, assignee. United States Patent US 7335771. 2008 Feb 26.
12. Pomel, V.; Klicic, J.; Covini, D.; Church, D. D.; Shaw, J. P.; Roulin, K.; Burgat-Charvilon, F.; Valognes, D.; Camps, M.; Chabert, C.; Gillieron, C.; Francon, B.; Perrin, D.; Leroy, D.; Gretener, D.; Nichols, A.; Vitte, P. A.; Carboni, S.; Rommel, C.; Schwarz, M. K.; Rückle, T. *J. Med. Chem.* **2006**, *49*, 3857.
13. (a) Roquet, S.; Cravino, A.; Leriche, P.; Alévêque, O.; Frère, P.; Roncali, J. *J. Am. Chem. Soc.* **2006**, *128*, 3459. (b) Thomas, K. R. J.; Hsu, Y. C.; Lin, J. T.; Lee, K. M.; Ho, K. C.; Lai, C. H.; Cheng, Y. M.; Chou, P. T. *Chem. Mater.* **2008**, *20*, 1830.
14. (a) Morley, J. O.; Push, D. *J. Chem. Soc. Faraday Trans.* **1991**, *87*, 3021. (b) Wu, I. Y.; Lin, J. T.; Li, C. S.; Tsai, C.; Wen, Y. S.; Hsu, C. C.; Yeh, F. F.; Liou, S. *Organometallics* **1998**, *17*, 2188.
15. March, J. *Advanced Organic Chemistry*, 4th ed.; Wiley: New York, U.S.A., 1992; p 45.
16. (a) Ramakishna, G.; Ghosh, H. N. *J. Phys. Chem. A* **2002**, *106*, 2545. (b) Wu, W.; Yang, J.; Hua, J.; Tang, J.; Zhang, L.; Long, Y.; Tian, H. *J. Mater. Chem.* **2010**, *20*, 1772.
17. Hwang, S.; Lee, J. H.; Park, C.; Lee, H.; Kim, C.; Park, C.; Lee, M. H.; Lee, W.; Park, J.; Kim, K.; Park, N. G.; Kim, C. *Chem. Commun.* **2007**, 4887.
18. (a) Hara, K.; Tachibana, Y.; Ohga, Y.; Shinpo, A.; Sugab, S.; Sayama, K.; Sugihara, H.; Arakawa, H. *Sol. Energy Mater. Sol. Cells* **2003**, *77*, 89. (b) Hara, K.; Sato, T.; Katoh, R.; Furube, A.; Ohga, Y.; Shinpo, A.; Suga, S.; Sayama, K.; Sugihara, H.; Arakawa, H. *J. Phys. Chem. B* **2003**, *107*, 597. (c) Kuang, D.; Walter, P.; Nüesch, F.; Kim, S.; Ko, J.; Comte, P.; Zakeeruddin, S. M.; Nazeeruddin, M. K.; Grätzel, M. *Langmuir* **2007**, *23*, 10906. (d) Hagberg, D. P.; Marinado, T.; Karlsson, K. M.; Nonomura, K.; Qin, P.; Boschloo, G.; Brinck, T.; Hagfeldt, A.; Sun, L. *J. Org. Chem.* **2007**, *72*, 9550.
19. Tae, E. L.; Lee, S. H.; Lee, J. K.; Yoo, S. S.; Kang, E. J.; Yoon, K. B. *J. Phys. Chem. B* **2005**, *109*, 22513.
20. Li, C.; Yang, X.; Chen, R.; Pan, J.; Tian, H.; Zhu, H.; Wang, X.; Hagfeldt, A.; Sun, L. *Sol. Energy Mater. Sol. Cells* **2007**, *91*, 1863.
21. (a) Ferrere, S.; Zaban, A.; Gregg, B. A. *J. Phys. Chem. B* **1997**, *101*, 4490. (b) Ferrere, S.; Gregg, B. A. *J. Phys. Chem. B* **2001**, *105*, 7602. (c) Ferrere, S.; Gregg, B. A. *New J. Chem.* **2002**, *26*, 1155. (d) Shibano, Y.; Umecyama, T.; Matano, Y.; Imahori, H. *Org. Lett.* **2007**, *9*, 1971. (e) Fortage, J.; Séverac, M.; Houarner-Rassin, C.; Pellegrin, Y.; Blart, E.; Odobel, F. *J. Photochem. Photobiol. A* **2008**, *197*, 156. (f) Jin, Y.; Hua, J.; Wu, W.; Ma, X.; Meng, F. *Synth. Met.* **2008**, *158*, 64.